Inorg. Chem. **2002**, *41*, 2672–2677

Mechanism of Silver-Promoted Ligand Metathesis in Square-Planar Complexes of d^8 Ions. Kinetics of Formation and Molecular Structures of a Trinuclear Intermediate $[(Me)(N–N)Pt(\mu\text{-}Cl)Ag(\mu\text{-}Cl)Pt(N–N)(Me)]^+$ and Its Dinuclear Evolution Product $[(Me)(N–N)Pt(\mu\text{-}Cl)Pt(N–N)(Me)]^+$ (N–N = ArN=C(Me)C(Me)=NAr, Ar = 2,6-(*i*-Pr)$_2$C$_6$H$_3$)

Vincenzo G. Albano,*,† Martino Di Serio,‡ Magda Monari,† Ida Orabona,‡ Achille Panunzi,‡ and Francesco Ruffo*,‡

Dipartimento di Chimica "G. Ciamician", Università di Bologna, via F. Selmi 2, I-40126 Bologna, Italy, and Dipartimento di Chimica, Università di Napoli "Federico II", Complesso Universitario di Monte S.Angelo, via Cintia, I-80126 Napoli, Italy

Received October 15, 2001

The silver-assisted ligand methatesis reaction involving a platinum(II) complex of formula [PtClMe(N,N-chelate)] with acetonitrile has been investigated. By using a suitably hindered N,N-chelate, an otherwise hardly detectable trinuclear species has been isolated and characterized through X-ray diffractometry. The trinuclear cation consists of two nearly orthogonal [PtCl(Me)(N,N-chelate)] square-planar units entrapping an Ag^+ cation through the chloride ligands that, acting as bidentate, form a linear $AgCl_2$ unit with two nonequivalent Ag–Cl bonds. The residual acidity of the silver cation is satisfied by one secondary Ag–Pt interaction [Ag–Pt(1) = 2.82 Å] in which the platinum atom acts as a donor. Kinetic studies have demonstrated that the silver assistance operates both through a simple associative step and through a pathway in which the above trinuclear complex is an active intermediate. In a noncoordinating solvent the latter species evolves with AgCl loss and formation of a dinuclear Pt,Pt complex showing a rare single chloride bridge.

Introduction

It is acknowledged[1] that the presence of a positive charge in a metal complex enhances its ability in promoting several organic reactions. Within d^8 ions this is testified by a significant number of examples,[1,2] spanning from the olefin polymerization catalyzed by monopositive Ni(II) and Pd(II) complexes[2a] to the nucleophilic activation of alkenes promoted by dipositive Pd(II) and Pt(II) centers.[1a] Therefore, several synthetic methods have been developed to prepare positively charged complexes, generally starting from the corresponding neutral species, which are often more stable and easy to handle. A widely used procedure is the halide abstraction by a silver salt in the presence of an incoming neutral L ligand (eq 1).[3]

This reaction is generally shifted toward the products by the low solubility of the silver halide in the reaction medium.

$$L'_nM{-}X + AgY + L = [L'_nM{-}L]^+Y^- + AgX \quad (1)$$

As a part of our research dealing with cationic olefin complexes of platinum(II),[4] we have recently described the preparation of new square-planar complexes of formula $[Pt(Me)(N,N\text{-chelate})(L)]^+$ (L = e.g. olefin or nitrile) by the

* To whom correspondence should be addressed. E-mail: vgalbano@ciam.unibo.it (V.G.A.); ruffo@unina.it (F.R.).
† Università di Bologna.
‡ Università di Napoli "Federico II".

(1) (a) Hahn, C.; Morvillo, P.; Vitagliano, A. *Eur. J. Inorg. Chem.* **2001**, 419−429. (b) Maresca, L.; Natile, G. *Comments Inorg. Chem.* **1994**, *16*, 95−112.
(2) (a) Ittel, S. D.; Johnson, L. K.; Brookhart, M. *Chem. Rev.* **2000**, *100*, 1169−1203. (b) Michelin, R. A.; Mozzon, M.; Bertani, R. *Coord. Chem. Rev.* **1996**, *147*, 299−338.
(3) Liston, D. J.; Lee, Y. J.; Scheidt, W. R.; Reed, C. A. *J. Am. Chem. Soc.* **1989**, *111*, 6643−6648.
(4) (a) Orabona, I.; Macchioni, A.; Ruffo, F.; Zuccaccia, C. *Organometallics* **1999**, *18*, 4367−4372. (b) Ganis, P.; Orabona, I.; Ruffo, F.; Vitagliano, A. *Organometallics* **1998**, *17*, 2646−2650. (c) Fusto, M.; Giordano, F.; Orabona, I.; Panunzi, A.; Ruffo, F. *Organometallics* **1997**, *16*, 5981−5987.

10.1021/ic011059p CCC: $22.00
Published on Web 04/19/2002

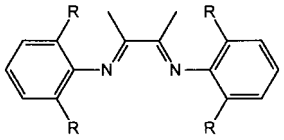

R= *i*-C_3H_7, **A**
R= H, **B**

Figure 1. Structure of ligands **A** and **B**.

just mentioned reaction (eq 2), where N,N-chelate is a bidentate nitrogen ligand such as **A** or **B** (Figure 1).

$$[PtCl(Me)(N,N\text{-chelate})]\ (\mathbf{I}) + AgY + L = [Pt(Me)(L)(N,N\text{-chelate})]^{+}Y^{-}\ (\mathbf{II}) + AgCl \quad (2)$$

Quite surprisingly, we have found that the type **I** compound of ligand **A** (**IA**) was resistant to undergo reaction 2, which could be successfully accomplished only by stirring the reaction mixture for several hours. It should be noted that **A** belongs to the class of axially hindered chelates which afford steric bulk above and below the coordination plane and, hence, inhibit associative processes.[2a] On the other hand, ligand **B** does not introduce substantial axial hindrance.

The dependence of the substitution rate from the steric hindrance of the chelate suggested that significant mechanistic insight into the silver-assisted metathesis reaction could be achieved on examining the above system.

Thus, we have undertaken a thorough investigation of reaction 2, which has allowed the isolation of an unusual trinuclear Pt,Ag,Pt complex (**IIIA**). The X-ray molecular structure has shown that this cationic compound consists of two square-planar moieties of type **I** linked by a chloro-bridged silver cation. A kinetic study has demonstrated that this polynuclear compound is one intermediate of reaction 2. Thus, the mechanism involves both a simple associative step assisted by coordination of the silver cation to the Pt−Cl bond and a more complicated pathway where the trinuclear species plays a key role.

Although previous studies already pointed out the active participation of the silver cation,[3,5] this is the first time where the kinetic data point to a reaction pathway more complicated than a simple bimolecular step.

Furthermore, when complex **IIIA** is allowed to slowly decompose in a noncoordinating solvent, loss of AgCl is observed with formation of a binuclear Pt,Pt complex (**VA**) that an X-ray diffraction study has shown to consist of two square-planar units linked by a rare Pt−Cl−Pt single chloride bridge.

Experimental Section

All experiments were carried out under nitrogen atmosphere using Schlenk techniques. Solvents and reagents were of AnalaR grade and were used without further purification, unless otherwise stated. THF was dried and distilled from Na/benzophenone. [PtCl(Me)(**A**)] and [PtCl(Me)(**B**)] were prepared according to literature procedures.[4c] ^{1}H NMR spectra were recorded on a Varian XL-200 spectrometer. $CDCl_3$ and a 20:3 mixture of CD_3NO_2/CD_3CN were used as solvents, and $CHCl_3$ (δ = 7.26) and CD_2HNO_2 (δ = 4.33) as internal standards. The following abbreviations were used for describing NMR multiplicities: s, singlet; d, doublet; t, triplet; h, heptet; m, multiplet. Infrared spectra were recorded on a JASCO FT-IR 430 spectrometer.

Synthesis of IIIA. Solid [PtCl(Me)(**A**)] (0.065 g, 0.10 mmol) was added to a stirred solution of $AgBF_4$ (0.020 g, 0.10 mmol) and acetonitrile (0.004 g, 0.10 mmol) in 1 mL of dry THF. After 5 min of stirring, the solvent was removed under vacuum. The red residue was extracted with dichloromethane and crystallized by slow addition of *n*-pentane (0.070 g, 82%). Crystals suitable for X-ray analysis were obtained from THF/diethyl ether. ^{1}H NMR ($CDCl_3$, 298 K): δ 7.29 (m, 6H, Ar), 2.92 (m, 4H, C*H*Me$_2$), 1.97 (s, 3H, N=CMe), 1.77 (s, 3H, N=CMe), 1.31 (d, 6H, CH*Me$_2$*), 1.26 (d, 6H, CH*Me$_2$*), 1.54 (d, 6H, CH*Me$_2$*), 1.49 (d, 6H, CH*Me$_2$*), 0.73 (s, 3H, $^3J_{HPt}$ 73 Hz, Pt−Me). IR (in KBr): ν 1100 cm^{-1} (br) (BF_4^-). Anal. Calcd for $C_{58}H_{86}AgBCl_2F_4N_4Pt_2$: C, 46.59; H, 5.80; N, 3.75. Found: C, 46.85; H, 5.63; N, 3.91.

Synthesis of IIB. Solid [PtCl(Me)(**B**)] (0.048 g, 0.10 mmol) was added to a stirred solution of $AgBF_4$ (0.020 g, 0.10 mmol) and acetonitrile (0.004 g, 0.10 mmol) in 1 mL of dry THF. After 5 min of stirring, the solvent was removed under vacuum and the yellow residue was extracted with dichloromethane. Removal of the solvent under vacuum afforded the complex in almost quantitative yield. ^{1}H NMR ($CDCl_3$, 298 K): δ 7.50 (m, 4H, Ar), 7.38 (d, 2H, Ar), 7.26 (t, 2H, Ar), 7.12 (d, 2H, Ar), 2.19 (s, 3H, N=CMe), 2.12 (s, 3H, N=CMe), 2.08 (s, 3H, $^4J_{HPt}$ 14 Hz, MeCN), 0.54 (s, 3H, $^3J_{HPt}$ 75 Hz, Pt−Me). Anal. Calcd for $C_{19}H_{22}BF_4N_3Pt$: C, 39.74; H, 3.86; N, 7.32. Found: C, 39.59; H, 3.81; N, 7.24.

Synthesis of VA. Complex **IIIA** (0.15 g, 0.10 mmol) was dissolved in 3 mL of chloroform. After 3 days AgCl was filtered out and the volume of the solution reduced under vacuum. Careful addition of diethyl ether afforded red crystals of product (0.11 g, 81%). Crystals suitable for X-ray analysis were obtained from chloroform/diethyl ether. ^{1}H NMR ($CDCl_3$, 298 K): δ 7.35−7.15 (m, 6H, Ar), 2.84 (m, 4H, C*H*Me$_2$), 1.79 (s, 3H, N=CMe), 1.62 (s, 3H, N=CMe), 1.19 (d, 6H, CH*Me$_2$*), 1.10 (d, 6H, CH*Me$_2$*), 1.05 (d, 6H, CH*Me$_2$*), 0.94 (d, 6H, CH*Me$_2$*), 0.66 (s, 3H, $^3J_{HPt}$ 72 Hz, Pt−Me). IR (in KBr): ν 1100 cm^{-1} (br) (BF_4^-). Anal. Calcd for $C_{58}H_{86}BClF_4N_4Pt_2$: C, 51.53; H, 6.41; N, 4.14. Found: C, 51.77; H, 6.30; N, 4.23.

Kinetic Measurements. A weighted amount of the appropriate platinum complex (**IA** or **IIIA**) was dissolved in 0.60 mL of a 20:3 mixture of CD_3NO_2/CD_3CN and immediately transferred in an NMR tube. Eventually, a known amount of $AgBF_4$ was dissolved in solution. NMR spectra of the reacting mixture were recorded at regular intervals of time at 303 K. The temperature was calibrated by using a separate methanol sample, according to a standard procedure. In all the experiments the reaction was complete within 30−90 min. The concentrations of the platinum species could be evaluated by integrating suitable separated peaks, i.e. the Pt−Me signals. ^{1}H NMR for **IIA** (20:3 CD_3NO_2/CD_3CN, 303 K): δ 7.45 (m, 6H, Ar), 3.10 (h, 1H, C*H*Me$_2$), 3.02 (h, 1H, C*H*Me$_2$), 2.18 (s, 3H, N=CMe), 2.16 (s, 3H, N=CMe), 1.40 (d, 6H, CH*Me$_2$*), 1.36 (d, 6H, CH*Me$_2$*), 1.25 (d, 6H, CH*Me$_2$*), 1.20 (d, 6H, CH*Me$_2$*), 0.52 (s, 3H, $^3J_{HPt}$ 81 Hz, Pt−Me).

X-ray Diffraction Experiments and Structure Determination of Cations IIIA and VA as $[BF_4]^-$ Salts. Crystal data and other experimental details for both species are reported in Table 1. The X-ray diffraction data were measured on a Bruker AXS SMART 2000 diffractometer, equipped with a CCD area detector, using Mo Kα radiation (λ = 0.710 73 Å) at room temperature. Cell dimensions and orientation matrixes were initially determined from least-

(5) Erickson, L. E.; Godfrey, M.; Larsen, R. G. *Inorg. Chem.* **1987**, *26*, 992−997.

Table 1. Crystal Data and Diffraction Experimental Details for Cations **IIIA** and **VA** in Their $[BF_4]^-$ Salts

formula	$C_{58}H_{86}AgBCl_2F_4N_4Pt_2 \cdot 0.5thf$	$C_{59}H_{86}BCl_4F_4N_4Pt_2$
fw	1547.1	1470.1
temp, K	293(2)	293(2)
λ, Å	0.710 73	0.710 73
cryst symmetry	triclinic	monoclinic
space group	$P\bar{1}$ (No. 2)	$P2_1/n$ (No. 14)
a, Å	10.5016(3)	16.170(1)
b, Å	17.9486(5)	24.522(1)
c, Å	18.7605(5)	18.464(1)
α, deg	109.921(1)	90
β, deg	90.684(1)	112.189(1)
γ, deg	91.212(1)	90
V, Å^3	3323.1(2)	6779.2(6)
Z	2	4
σ_{calcd}, Mg m^{-3}	1.510	1.440
μ(Mo Kα), mm^{-1}	4.620	4.327
$R_1(F)$,[a] $wR_2(F^2)$[b]	0.0419, 0.0947	0.0374, 0.0728

[a] $R_1 = \Sigma||F_o| - |F_c||/\Sigma|F_o|$. [b] $wR_2 = [\Sigma w(F_o^2 - F_c^2)^2/\Sigma w(F_o^2)^2]^{1/2}$, where $w = 1/[\sigma^2(F_o^2) + (aP)^2 + bP]$, where $P = (F_o^2 + 2F_c^2)/3$.

squares refinements on reflections measured in three sets of 20 exposures collected in three different ω regions and eventually refined against all reflections. Full spheres of the diffraction space were measured by 0.3° ω steps, 40 s exposures, and the sample−detector distance kept at 5.0 cm. Intensity decay was monitored by recollecting the initial 50 frames at the end of each data collection and analyzing the duplicate reflections. The collected frames were processed for integration by using the program SAINT, and an empirical absorption correction was applied using SADABS[6] on the basis of the Laue symmetry of the reciprocal space. The structures were solved by direct methods (SIR 97)[7] and subsequent Fourier syntheses and refined by full-matrix least-squares calculations on F^2 (SHELXTL)[8] using anisotropic thermal parameters for all non-hydrogen atoms. The hydrogen atoms were located experimentally, but their positions were idealized and refined riding the pertinent carbon atoms [C(sp^3)−H = 0.98, C(sp^2)−H = 0.93 Å].

The refinement of the structure model of **VA** was straightforward, and the final difference electron density map was featureless. On the contrary, the Fourier map for **IIIA** showed some significant residual peaks of electron density. Two peaks were located in the vicinity of the silver cation, and three were grouped around the inversion center at 0.5, 0.5, 0.5, forming a sort of cyclohexane. The latter were reasonably explained as a tetrahydrofuran molecule exhibiting a double image for the oxygen atom and single images for the CH_2 groups. The rationalization of the stronger peaks (4.5 and 1.8 e Å^{-3}) proved more tricky because they were placed at 1.87 Å from each other and at 1.03 and 1.18 Å from Ag, respectively. The distances from Ag were clearly inconsistent with the position of this atom and were tentatively rationalized as alternative positions of the silver cation. A refinement of the site occupation factors afforded the following values: Ag(a) 0.87; Ag(b) 0.09; Ag(c) 0.04. An explanation of the reason the silver cation resulted as split over three sites came from an analysis of the bonding distances of its fainter images (Å): Ag(b)−Cl(1), 2.23; Ag(b)−C(2)(methyl), 2.56; Ag(c)−Cl(2), 2.48; Ag(c)−C(1)(methyl), 2.68. The supposed silver−methyl contacts would become chemically acceptable if they actually were silver−chloride interactions.

(6) Sheldrick, G. M. *SADABS, Program for empirical absorption correction*; University of Göttingen: Göttingen, Germany, 1996.
(7) Altomare, A.; Burla, M. C.; Camalli, M.; Cascarano, G. L.; Giacovazzo, C.; Guagliardi, A.; Moliterni, A. G. G.; Polidori, G.; Spagna, R. *J. Appl. Crystallogr.* **1999**, *32*, 115−119.
(8) Sheldrick, G. M. *SHELXTLplus Version 5.1 (Windows NT version)-Structure Determination Package*; Bruker Analytical X-ray Instruments Inc.: Madison, WI, 1998.

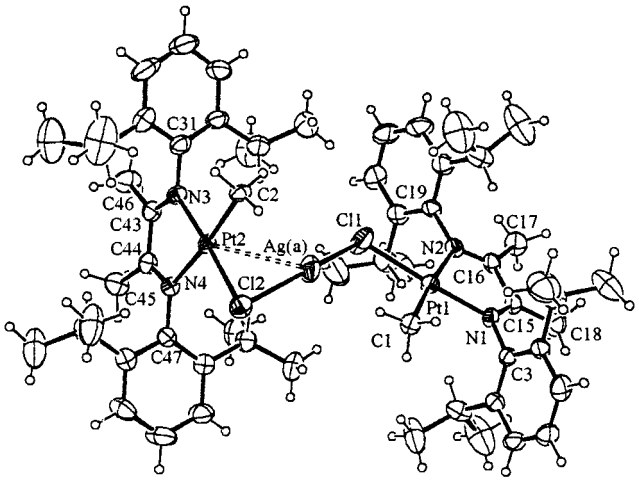

Figure 2. ORTEP drawing of cation **IIIA** as determined by X-ray diffraction in its $[BF_4]^-$ salt. Thermal ellipsoids are drawn at 30% of the probability level. For the sake of clarity, the atom labeling has been omitted where not necessary.

Therefore, disorder was postulated in the crystal at the level of the molecular units; i.e., parts of the platinum complexes were rotated or reflected in accord with the symmetry of the diimine ligands leaving these ligands substantially unmoved but determining Cl/Me scrambling [9% around Pt(1) and 4% around Pt(2)]. As a consequence, the silver cation had to move in accord with the displacements of its ligands producing the observed multiple images and allowing one to detect and measure the phenomenon that otherwise would have remained unnoticed.

Results and Discussion

Isolation and X-ray Solid-State Structure of the Trinuclear Complex Cation [(Me)(N−N)Pt(μ-Cl)Ag(μ-Cl)Pt(N−N)(Me)]$^+$ (IIIA). The study of the mechanism of reaction 2 has been accomplished by using MeCN as incoming L ligand and $AgBF_4$ as the source of Ag^+:

$$[PtCl(Me)(\mathbf{A})]\,(\mathbf{IA}) + AgBF_4 + MeCN = [Pt(Me)(\mathbf{A})(MeCN)]\,[BF_4]\,(\mathbf{IIA}) + AgCl \quad (3)$$

When solid [PtCl(Me)(**A**)] (**IA**) is added to a solution in dry THF containing 1 equiv of both $AgBF_4$ and MeCN, immediate formation of a clear red solution ensues. Slow formation of AgCl is subsequently observed. After 24 h the solvent is removed under vacuum and product **IIA** can be extracted in quantitative yield with dichloromethane. Alternatively, removal of the solvent from the early-formed red solution affords an orange solid, which can be crystallized as orange needles (**IIIA**). The ^{1}H NMR spectrum of these crystals discloses the presence of a single species. Elemental analyses reveal the presence of silver in the molecule, while the IR spectrum shows the presence of $[BF_4]^-$. The data suggest a cationic structure where both Pt and Ag are present, possibly linked via a Cl bridge. This hypothesis has been confirmed by an X-ray diffraction experiment.

The molecular structure of **IIIA**, as determined in its $[BF_4]^-$ salt, is shown in Figure 2, and selected bond distances and angles are reported in Table 2. The cation consists of two [PtCl(Me)(**A**)] planar molecules and an Ag^+ cation

Table 2. Selected Bond Lengths (Å) and Angles (deg) for **IIIA**

Pt(1)−N(1)	2.006(2)	N(2)C(16)	1.282(4)
Pt(1)−N(2)	2.091(2)	N(2)C(19)	1.420(3)
Pt(1)−C(1)	2.064(3)	N(3)−C(43)	1.288(4)
Pt(2)−N(3)	2.016(2)	N(3)−C(31)	1.422(3)
Pt(2)−N(4)	2.094(2)	N(4)−C(44)	1.284(4)
Pt(2)−C(2)	2.100(3)	N(4)−C(47)	1.417(3)
Pt(2)−Cl(2)	2.298(1)	C(15)−C(16)	1.491(4)
Pt(2)−Ag(a)	2.895(1)	C(16)−C(17)	1.498(4)
Pt(1)−Cl(1)	2.291(1)	C(15)−C(18)	1.470(4)
Ag(a)−Cl(1)	2.398(1)	C(43)−C(44)	1.480(5)
Ag(a)−Cl(2)	2.471(1)	C(43)−C(46)	1.489(5)
N(1)−C(15)	1.290(4)	C(44)−C(45)	1.496(5)
N(1)−C(3)	1.419(3)		
Pt(1)−Cl(1)−Ag(a)	113.34(5)	Pt(2)−Cl(2)−Ag(a)	74.64(3)
N(1)−Pt(1)−N(2)	77.2(1)	N(3)−Pt(2)−N(4)	77.3(1)
N(1)−Pt(1)−C(1)	98.2(1)	N(3)−Pt(2)−C(2)	97.2(1)
C(1)−Pt(1)−Cl(1)	88.1(1)	Cl(1)−Ag(a)−Cl(2)	164.87(5)

entrapped between the chloride ligands in an almost linear $AgCl_2$ unit [Ag(a)−Cl(1) = 2.398(1), Ag(a)−Cl(2) = 2.471(1) Å, Cl(1)−Ag(a)−Cl(2) = 164.87(5)°].[9] The resulting trinuclear supercation adopts an asymmetric overall conformation. As a consequence, Ag^+ is differently positioned with respect to the two [PtCl(Me)(**A**)] moieties. It sits in the coordination plane of Pt(1) (distance from the average plane 0.15 Å) and is well out of the coordination plane of Pt(2) [dihedral angle between coordination and Pt(2)Cl(2)Ag(a) planes 71.26(6)°]. In this geometry Ag^+ falls within bonding distance of Pt(2) [2.895(1) Å] and remains far apart from Pt(1) [3.84 Å]. An analysis of the Pt−Cl−Ag(a) angles [Pt(1)−Cl(1)−Ag(a) = 113.34(4)°, Pt(2)−Cl(2)−Ag(a) = 74.64(3)°] strongly suggests an attractive Pt(2)···Ag(a) interaction; otherwise more balanced values would have been observed. The consistence of the dative Pt(2)→Ag(a) interaction could have been estimated by comparing the corresponding bond distances around Pt(2) and Pt(1). Unfortunately an accurate analysis of the electron density map has given evidence of some methyl−chloride disorder [ca. 9% and 4% scrambling around Pt(2) and Pt(1), respectively]. Therefore we are discussing the cation conformation of highest weight (ca. 87%) and the platinum−ligand bond distances are weighted average values over the different molecules packed in the crystal and cannot be used for detecting differences in electron saturation of the two platinum atoms. The degree of the Pt(2)→Ag(a) interaction could also be evaluated from the displacements of the Pt atoms out of their coordination planes. Actually both atoms are strictly in plane (deviation 0.001 Å), and therefore, the Pt(2)···Ag(a) interaction is a weak one and the asymmetric conformation of the entire molecule is motivated more by the optimization of the molecular bulk than by the formation of some metal−metal bond. Platinum−silver interactions are not a novelty,[10] but the present cation displays the peculiarity of the neutral nature of the platinum units. A comparable stereochemical situation has been found in the polymeric complex $[PtAgCl_2(C_6Cl_5)(PPh_3)]$,[11] even though this species is substantially different from an electronic point of view, the platinum complex being an anion.

Scheme 1

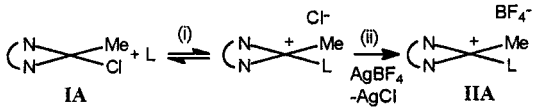

Scheme 2

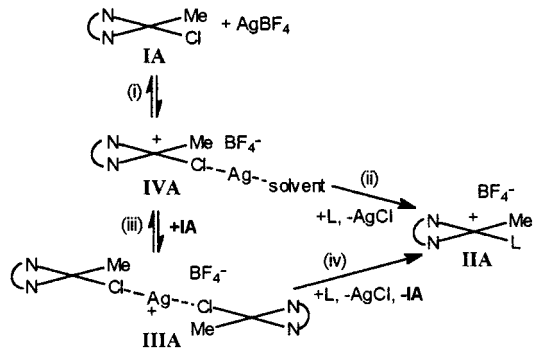

Although the diimine ligands are not appreciably affected by disorder, their dominating contribution in determining the molecular shape, together with their ability to conform to C_2, C_s, or C_{2v} idealized symmetries, is at the origin of the partial disorder of the chloride−methyl groups. The packing interactions do not completely discriminate molecules rotated according to the symmetry of the dominating ligand, and some Cl/Me mixing takes place in the crystal. Actually the ligand at Pt(1) adopts an idealized C_{2v} symmetry, while that at Pt(2) is better described by a C_s symmetry with the mirror plane orthogonal to the coordination plane. The multisite locations of the chloride ligands generate corresponding displacements of the silver cation, but the Coulombic component of the packing energy seems little affected. In fact Ag^+ is incapsulated in the core of a large molecular assemblage and is far away from the $[BF_4]^-$ counterions (shortest Ag(a)···F distance 9.82 Å). Anyway the increase of configurational entropy generated by the disorder is beneficial to the crystal stability.

Kinetic Studies. The successful isolation of the polynuclear species **IIIA** has stimulated us to gain insight into the mechanism of reaction 3. Previous related works[3,5] suggest that silver may have either a simple scavenger role (Scheme 1) or a more active function (Scheme 2). In the former circumstance, the incoming MeCN ligand would substitute the chloride with formation of the cationic $[Pt(Me)(\mathbf{A})(MeCN)]^+Cl^-$ intermediate (reaction i in Scheme 1), and then AgCl would precipitate (reaction ii). In the latter case, the Ag^+ ion would first link the metal-bonded chloride of **IA** (reaction i in Scheme 2) by forming the undetected **IVA** binuclear cation, which may evolve into the final product through reaction ii of Scheme 2. However, our results suggest that this Pt,Ag complex is able to interact with a second molecule of **IA** with formation of the isolated trinuclear complex **IIIA** (reaction iii). Thus, the mechanistic investigation must take into account the possibility that also **IIIA** may afford the final product **IIA** (reaction iv). The

(9) For the meaning of the labels on silver ion, see the Experimental Section.
(10) Usòn, R.; Forniés, J. *Inorg. Chim. Acta* **1992**, *198*−*200*, 165−177.
(11) Usòn, R.; Forniés, J.; Tomàs, M.; Ara, I. *Inorg. Chem.* **1994**, *33*, 4023−4028.

relative rates of reactions ii and iv can indicate if **IIIA** is actually an intermediate of reaction 3.

Several kinetic experiments have been performed aiming to discriminate among the plausible mechanisms (see Table S1 of the Supporting Information). All runs have been performed at 303 K, using a mixture of CD_3NO_2 and CD_3CN (20:3) as solvent (0.60 mL) and different initial amounts of **IA**, **IIIA**, and $AgBF_4$.

The experimental data of runs performed at different silver concentrations clearly indicate that the reaction rate strongly depends on the concentration of this ion. Therefore, the mechanism shown in Scheme 1 is certainly not operating, since silver would take part only in reaction ii, i.e. in the precipitation of the silver chloride that surely cannot be the slow reaction of the mechanism. This agrees with previous results on a related system.[5]

Once clarified that the role played by Ag^+ is not a passive one, the mechanism proposed in Scheme 2 has been investigated. Reactions i and iii can be considered as fast equilibria. Actually, even at low temperatures (223 K) average NMR signals are observed for the involved complexes.[12] On the other hand, the slow reactions of the mechanism can be considered reactions ii and iv. In fact, success in isolating a stable complex such as **IIIA** undoubtedly stems from the ability of the chelate to inhibit associative processes;[2a] i.e., the hindrance above and below the coordination plane inhibits the approach of acetonitrile. In keeping with this hypothesis, when reaction 3 is performed on the complex of the poorly crowded ligand **B**, the cationic product [Pt(Me)(MeCN)(**B**)]BF_4 (**IIB**) is rapidly formed.

Therefore, the concentration of **IIA** and of all the species containing Ag (C_{Ag}) is given by the numerical integration of the following equations:

$$d[\mathbf{IIA}]/dt = r_{ii} + r_{iv} \quad (4)$$

$$dC_{Ag}/dt = -r_{ii\,-} r_{iv} \quad (5)$$

Since CD_3CN is in wide excess, the rates of reactions ii and iv are surely of order 0 for this reagent, while they will be dependent on the concentration of **IVA** and **IIIA**:

$$r_{ii} = k_{ii}[\mathbf{IVA}] \quad (6)$$

$$r_{iv} = k_{iv}[\mathbf{IIIA}] \quad (7)$$

The concentrations of **IVA** and **IIIA** are given by the solution of the mass balances (8) and (9), where C°_{Pt} is the initial total platinum concentration. By using the equilibrium equations 10 and 11, it is obtained

$$[\mathbf{IA}] + [\mathbf{IIA}] + 2[\mathbf{IIIA}] + [\mathbf{IVA}] = C^\circ_{Pt} \quad (8)$$

$$[Ag^+] + [\mathbf{IIA}] + [\mathbf{IIIA}] + [\mathbf{IVA}] = C_{Ag} \quad (9)$$

$$K(e_i) = [\mathbf{IVA}]/([\mathbf{IA}][Ag^+]) \quad (10)$$

$$K(e_{iii}) = [\mathbf{IIIA}]/([\mathbf{IA}][\mathbf{IVA}]) \quad (11)$$

The equations 8−11 correspond to a nonlinear equations system that must be solved before every integration step. The parameters of the model [$K(e_i)$, $K(e_{iii})$, k_{ii}, and k_{iv}] can be obtained by nonlinear regression of the model on the experimental data of the runs reported in Table S1.

The model described above is general and foresees the possibility to arrive to **IIA** either through the dinuclear **IVA** or the trinuclear **IIIA**. Possible particular cases can be devised as, for instance, a mechanism in which only **IIIA** (mechanism 2a, $k_{ii} = 0$) or only **IVA** (mechanism 2b, $k_{iv} = 0$) evolves to **IIA** or that **IVA** and **IIIA** have comparable reactivity (mechanism 2c, $k_{ii} \sim k_{iv}$). The last assumption is the most reasonable because species **IIIA** and **IVA** exhibit similar steric hindrance. Nevertheless, to discriminate between the three models, these have all been submitted to nonlinear regression[13] on the experimental data. In Figure S5 of the Supporting Information the deviations between calculated and experimental values can be appreciated. Model 2c provides lower deviations and, on the other hand, also a better correlation index (99.40 against 97.97 of mechanism 2a and 97.35 of mechanism 2b). In Figures S1−S4 the accords obtained with the parameters of the model 2c determined by regression [$K(e_i) = 6.6 \pm 1.5$ mL/mmol, $K(e_{iii}) = 71 \pm 25$ mL/mmol, $k_{ii} = k_{iv} = 0.070 \pm 0.010$ 1/min] between experimental data and calculated values can be appreciated. The same result was obtained when the calculations were performed by allowing different values for k_{ii} and k_{iv}.

The analysis on the models shows that both **IVA** and **IIIA** evolve to **IIA**, and therefore, they are both intermediates of the silver salt metathesis under investigation.

X-ray Structure of the Dinuclear Cation [(Me)(N−N)Pt(μ-Cl)Pt(N−N)(Me)]$^+$ (VA) Obtained from IIIA by AgCl Loss. Complex **IIIA** has revealed to be unstable in deuteriochloroform solution. AgCl quantitatively precipitates within few days with formation of a new complex (**VA**). Also in this case the molecular structure has been determined by X-ray diffraction and has clearly revealed that cation **VA** is the product of AgCl elimination from **IIIA**. The molecule is illustrated in Figure 3, and selected bond distances and angles are reported in Table 3. The stereogeometry of the cation shows the presence of two equivalent square-planar Pt(II) units sharing the chloride ligand. The molecular conformation is determined by the need to avoid close intraligand contacts, especially between the methyl ligands and the bulky 2,5-(i-Pr)$_2$C$_6$H$_3$ groups that are placed almost orthogonally to the PtN_2C_2 chelate rings. The Pt(1)−Cl−Pt(2) angle is obtuse [119.39(5)°] and the Pt(1)···Pt(2) contact quite long [3.965(1) Å]. The two square moieties are flat (deviations from the average planes in the range ±0.02 Å) and symmetrically rotated out of the Pt(1)ClPt(2) plane (±37.5°); therefore, the cation as a whole conforms to a C_2 idealized symmetry. The bond distances in the two chemically equivalent units are equal within experimental

(12) The strong MLCT band displayed by the involved species and precipitation of AgCl prevented an equilibrium study through UV−vis spectroscopy.

(13) Buzzi Ferraris, G. *Ing. Chim. Ital.* **1968**, *12*, 171−176.

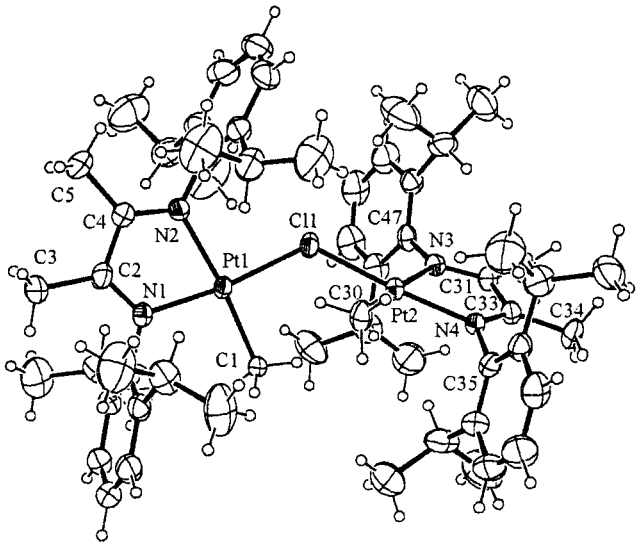

Figure 3. ORTEP drawing of cation **VA** as determined by X-ray diffraction in its $[BF_4]^-$ salt. Thermal ellipsoids are at the 30% probability level. For the sake of clarity, the atom labeling has been omitted where not necessary.

Table 3. Selected Bond Lengths (Å) and Angles (deg) for VA

Pt(1)−Cl(1)	2.296(1)	C(2)−C(4)	1.479(6)
Pt(2)−Cl(1)	2.296(1)	C(2)−C(3)	1.515(6)
Pt(1)−N(1)	1.990(3)	C(4)−C(5)	1.503(6)
Pt(1)−N(2)	2.091(3)	N(1)−C(18)	1.413(4)
Pt(2)−N(3)	2.103(3)	N(2)−C(6)	1.410(4)
Pt(2)−N(4)	2.000(3)	N(3)−C(31)	1.285(5)
Pt(1)−C(1)	2.069(4)	N(4)−C(33)	1.281(5)
Pt(2)−C(30)	2.068(4)	C(31)−C(33)	1.484(5)
N(1)−C(2)	1.288(5)	N(3)−C(47)	1.426(4)
N(2)−C(4)	1.289(5)	N(4)−C(35)	1.426(4)
Pt(1)···Pt(2)	3.965(3)		
Pt(1)−Cl(1)−Pt(2)	119.39(5)	N(1)−Pt(1)−Cl(1)	173.0(1)
N(1)−Pt(1)−N(2)	78.0(1)	N(4)−Pt(2)−Cl(1)	172.5(1)
N(3)−Pt(2)−N(4)	77.8(1)	Cl(1)−Pt(1)−C(1)	90.3(1)
N(1)−Pt(1)−C(1)	96.5(1)		

errors (see Table 3), and the average values of the platinum−ligand interactions are as follows (Å): Pt−Cl = 2.296(1); Pt−C(methyl) = 2.068(4); Pt−N = 1.995(5) and 2.097(5) for the nitrogens trans to the chloride and methyl groups, respectively. These values agree well with those recently reported for the mononuclear species [PtClMe(ArN=CHCH=NAr)] (Ar = 2-($MeOCH_2$)-4,6-*t*-BuC_6H_2) (Å): Pt−Cl = 2.283(3); Pt−C(methyl) = 2.053(10); Pt−N = 1.994(9) and 2.122(9).[14] Also interesting is a comparison with the stereochemically more similar cation [Pt_2(*μ*-Cl)(*S*,*S*-*trans*-1-(N=CH(C_6H_4)-2-(N=CHPh)C_6H_{10})$_2$]$^+$.[15] The most significant difference concerns the orientations of the square-planar moieties in the latter that, in contrast to the skewed conformation in **VA**, feature an almost antiparallel arrangement accompanied by a short Pt···Pt contact [2.9696(6) Å], an acute Pt−Cl−Pt angle [77.48(9)°], and significant displacements of the bridging chloride ligand out of the coordination planes. We must conclude that this kind of conformation is energetically favored but not accessible to the title cation because of the cumbersome substituted aryl appendages. The platinum−ligand bonds in the two species exhibit similar trends except for the Pt−Cl interactions (average values 2.296(1) Å in **VA** and 2.372(5) Å in the other cation) as a consequence of the bond strain originated by the conformation of the cation.

A database search has revealed no molecule of similar structure except the palladium cation [Pd_2(*μ*-Cl){C_6H_3-(CH_2NMe_2)$_2$-o,o′}$_2$]$^+$,[16] whose overall conformation is similar to that of the present cation, despite significant differences in bond values, due to a nonequivalent bond disposition in the coordination plane.

Conclusions

This study provides a detailed investigation on the mechanism of one of the most widely used inorganic reactions, i.e. the silver-assisted methatesis reaction:

$$L'_nM{-}X + AgY + L = [L'_nM{-}L]^+Y^- + AgX$$

The presence of an axially hindered N,N-chelate in the coordination sphere of a Pt(II) complex has allowed the isolation and crystallization of the trinuclear Pt,Ag,Pt cation **IIIA**, whose structural features have been disclosed by an X-ray diffraction study. A kinetic study has clearly confirmed the involvement of **IIIA** in the reaction mechanism, which therefore consists of two parallel pathways. The first one involves formation of a dinuclear Pt,Ag intermediate, as already suggested in previous related studies.[3,5] Alternatively, this latter species can afford the trinuclear intermediate **IIIA**, which also can give rise to the final cationic product.

In a noncoordinating solvent, the trinuclear complex decomposes with AgCl loss and formation of a rare example of single chloro-bridged Pt,Pt dimer (**VA**).

Acknowledgment. The authors thank the Consiglio Nazionale delle Ricerche, the MURST (Programmi di Ricerca Scientifica di Rilevante Interesse Nazionale, Cofinanziamento 2000-2001), and the Centro Interdipartimentale di Metodologie Chimico-Fisiche, Università di Napoli "Federico II", for NMR facilities.

Supporting Information Available: A table of kinetic runs, figures showing the accord between the kinetic model and the experimental data, and X-ray crystallographic files in CIF format for the structure of complexes **IIIA** and **VA**. This material is available free of charge via the Internet at: http://pubs.acs.org.

IC011059P

(14) Yang, K.; Lachicotte, R. J.; Eisenberg, R. *Organometallics* **1998**, *17*, 5102−5113.

(15) Baar, C. R.; Jenkins, H. A.; Jennings, M. C.; Yap, G. P. A.; Puddephatt, R. J. *Organometallics* **2000**, *19*, 4870−4877.

(16) Terheijden, J.; van Koten, G.; Grove, D. M.; Vrieze, K.; Spek, A. L. *J. Chem. Soc., Dalton Trans.* **1987**, 1359−1366.